First Light for GRAVITY: A New Era for Optical Interferometry

GRAVITY Collaboration:

Roberto Abuter[8], Matteo Accardo[8], António Amorim[6], Narsireddy Anugu[7], Gerardo Ávila[8], Myriam Benisty[5], Jean-Philippe Berger[5], Nicolas Blind[9], Henri Bonnet[8], Pierre Bourget[8], Wolfgang Brandner[3], Roland Brast[8], Alexander Buron[1], Frédéric Cassaing[10], Frédéric Chapron[2], Élodie Choquet[2], Yann Clénet[2], Claude Collin[2], Vincent Coudé du Forestol[2], Willem-Jan de Wit[8], Casey Deen[1], Françoise Delplancke-Ströbele[8], Roderick Dembet[8], Frédéric Derie[8], Jason Dexter[1], Gilles Duvert[5], Monica Ebert[3], Andreas Eckart[4,13], Frank Eisenhauer[1], Michael Esselborn[8], Pierre Fédou[2], Gert Finger[8], Paulo Garcia[7], Cesar Enrique Garcia Dabo[8], Rebeca Garcia Lopez[3], Feng Gao[1], Éric Gendron[2], Reinhard Genzel[1,15], Stefan Gillessen[1], Frédéric Gonté[8], Paulo Gordo[6], Marion Grould[2], Ulrich Grözinger[3], Sylvain Guieu[5,8], Pierre Haguenauer[8], Oliver Hans[1], Xavier Haubois[8], Marcus Haug[1,8], Frank Haußmann[1], Thomas Henning[3], Stefan Hippler[3], Matthew Horrobin[4], Armin Huber[3], Zoltan Hubert[2], Norbert Hubin[8], Christian A. Hummel[8], Gerd Jakob[8], Lieselotte Jochum[8], Laurent Jocou[5], Martina Karl[1], Andreas Kaufer[8], Stefan Kellner[1,13], Sarah Kendrew[3,11], Lothar Kern[8], Pierre Kervella[2,12], Mario Kiekebusch[8], Ralf Klein[3], Johan Kolb[8], Martin Kulas[3], Sylvestre Lacour[2], Vincent Lapeyrère[2], Bernard Lazareff[5], Jean-Baptiste Le Bouquin[5], Pierre Léna[2], Rainer Lenzen[3], Samuel Lévêque[8], Magdalena Lippa[1], Yves Magnard[5], Leander Mehrgan[8], Marcus Mellein[3], Antoine Mérand[8], Javier Moreno-Ventas[3], Thibaut Moulin[5], Eric Müller[3,8], Friedrich Müller[3], Udo Neumann[3], Sylvain Oberti[8], Thomas Ott[1], Laurent Pallanca[8], Johana Panduro[3], Luca Pasquini[8], Thibaut Paumard[2], Isabelle Percheron[8], Karine Perraut[5], Guy Perrin[2], Pierre-Olivier Petrucci[5], Andreas Pflüger[1], Oliver Pfuhl[1], Thanh Phan Duc[8], Philipp M. Plewa[1], Dan Popovic[8], Sebastian Rabien[1], Andrés Ramírez[8], Jose Ramos[3], Christian Rau[1], Miguel Riquelme[8], Gustavo Rodríguez-Coira[2], Ralf-Rainer Rohloff[3], Alejandra Rosales[1], Gérard Rousset[2], Joel Sanchez-Bermudez[3], Sylvia Scheithauer[3], Markus Schöller[8], Nicolas Schuhler[8], Jason Spyromilio[8], Odele Straub[2], Christian Straubmeier[4], Eckhard Sturm[1], Marcos Suarez[8], Konrad R. W. Tristram[8], Noel Ventura[5], Frédéric Vincent[2], Idel Waisberg[1], Imke Wank[4], Felix Widmann[1], Ekkehard Wieprecht[1], Michael Wiest[4], Erich Wiezorrek[1], Markus Wittkowski[8], Julien Woillez[8], Burkhard Wolff[8], Senol Yazici[1,4], Denis Ziegler[2], Gérard Zins[8]

[1]Max Planck Institute for Extraterrestrial Physics, Garching, Germany; [2]LESIA, Observatoire de Paris, PSL Research University, CNRS, Sorbonne Universités, UPMC Université Paris 6, Université Paris Diderot, Sorbonne Paris Cité, France; [3]Max Planck Institute for Astronomy, Heidelberg, Germany; [4]I. Physikalisches Institut, University of Cologne, Germany; [5]Institut de Planétologie et d'Astrophysique de Grenoble (IPAG), Université Grenoble Alpes, CNRS, IPAG, France; [6]CENTRA — Universidade de Lisboa — Faculdade de Ciências, Portugal; [7]CENTRA — Universidade do Porto — Faculdade de Engenharia, Portugal; [8]ESO; [9]Observatoire de Genève, Université de Genève, Switzerland; [10]ONERA, The French Aerospace Lab, Châtillon, France; [11]European Space Agency, Space Telescope Science Institute, Baltimore, USA; [12]Unidad Mixta Internacional Franco-Chilena de Astronomía (CNRS UMI 3386), Departamento de Astronomía, Universidad de Chile, Santiago, Chile; [13]Max Planck Institute for Radio Astronomy, Bonn, Germany; [14]Leiden Observatory, The Netherlands; [15]Department of Physics, University of California, Berkeley, USA

With the arrival of the second generation instrument GRAVITY, the Very Large Telescope Interferometer (VLTI) has entered a new era of optical interferometry. This instrument pushes the limits of accuracy and sensitivity by orders of magnitude. GRAVITY has achieved phase-referenced imaging at approximately milliarcsecond (mas) resolution and down to ~ 100-microarcsecond astrometry on objects that are several hundred times fainter than previously observable. The cutting-edge design presented in Eisenhauer et al. (2011) has become reality. This article sketches out the basic principles of the instrument design and illustrates its performance with key science results obtained during commissioning: phase-tracking on stars with K ~ 10 mag, phase-referenced interferometry of objects fainter than $K \geq 17$ mag, minute-long coherent integrations, a visibility accuracy of better than 0.25 %, and spectro-differential phase and closure phase accuracy better than 0.5 degrees, corresponding to a differential astrometric precision of a few microarcseconds (µas).

GRAVITY was developed in a collaboration between the Max Planck Institute for Extraterrestrial Physics, LESIA of Observatoire de Paris/CNRS/UPMC/Université Paris Diderot and IPAG of Université Grenoble Alpes/CNRS, the Max Planck Institute for Astronomy, the University of Cologne, CENTRA–Centro Multidisciplinar de Astrofísica (Lisbon and Porto) and ESO.

GRAVITY was shipped to Paranal in July 2015 (Figures 1 and 2). After roughly one year of installation and commissioning, the instrument was offered to the scientific community for the first time in October 2016. The observations we report here include objects and results that were out of reach for any previous interferometric instrument. Most notable are observations of the Galactic Centre black hole Sagittarius A* (Sgr A*) and the nearby star S2 (Figure 3); the micro-quasar SS 433; and 50-microseconds accuracy astrometry of the M-dwarf binary system GJ 65. More details about GRAVITY and early commissioning results can be found in GRAVITY Collaboration (2017 a, b, c and d).

Phase referencing optical interferometry for the VLTI

As part of GRAVITY, each of the four 8.2-metre Unit Telescopes (UT) has been equipped with a Coudé Infrared Adaptive Optics (CIAO) system, which corrects atmospheric perturbations and stably injects the light from two adjacent astrophysical objects into optical fibres. Two fibres per telescope feed two integrated optics beam combiners: one for each object. Each beam combiner pairwise combines the telescopes and samples the resulting six fringe patterns at four phase-shifted locations. Those 24 outputs are dispersed by a spectrometer and imaged onto a detector. One of the two beam combiners serves as a fringe-tracker. It is equipped with a low-resolution spectrometer and a fast camera optimised to measure the fringe phase at kHz frequency. The fringe-tracker measures and corrects atmospheric piston perturbations in real time, which permits long integration times on the second beam combiner.

The active stabilisation of the science channel allows the integration time to be increased from a few milliseconds (atmospheric coherence time) to hundreds of seconds. The resulting leap in sensitivity opens up a wide range of applications, from very faint targets at low spectral resolution to moderately bright targets at high spectral resolution. Furthermore, GRAVITY provides dual-field astrometry by precisely measuring the optical delay between two distinct objects with a dedicated metrology system. This yields object separations with an exquisite accuracy of a few tens of µas.

Both single-field (where a beam splitter injects the light from a single object into the two fibres) and dual-field modes are offered to the community, with a spectral resolution up to 4000 and a limiting magnitude of $K = 8$ in single-field mode using the 1.8-metre Auxiliary Telescopes (ATs) and $K = 10$ on the 8-metre UTs depending on weather conditions. In dual-field mode, the offered limiting magnitude is 0.5 magnitudes fainter on the fringe-tracker, and 3.5 magnitudes on the science channel. Dual-field astrometry is still under commissioning. The first observations show residuals as low as 50 µas when following objects over several months.

Figure 1. After ten years of design and realisation in Europe, GRAVITY was shipped to Chile and brought up to Cerro Paranal in these two trucks in July 2015.

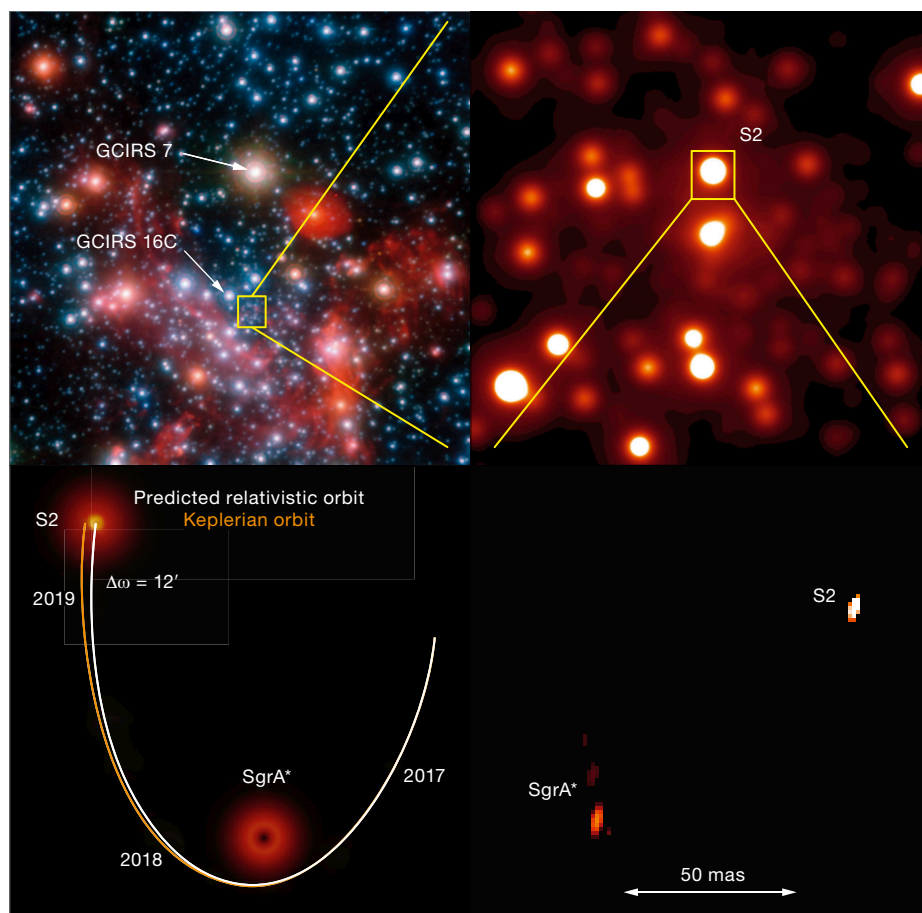Figure 2. GRAVITY in the integration hall immediately after shipment.

Figure 3. Top left: The central 20 arcseconds in the Galactic Centre with the adaptive optics and fringe-tracking reference stars. Top right: The central arcsecond as seen with the VLT instrument NAOS-CONICA (NACO). Bottom left: The shift between the predicted Keple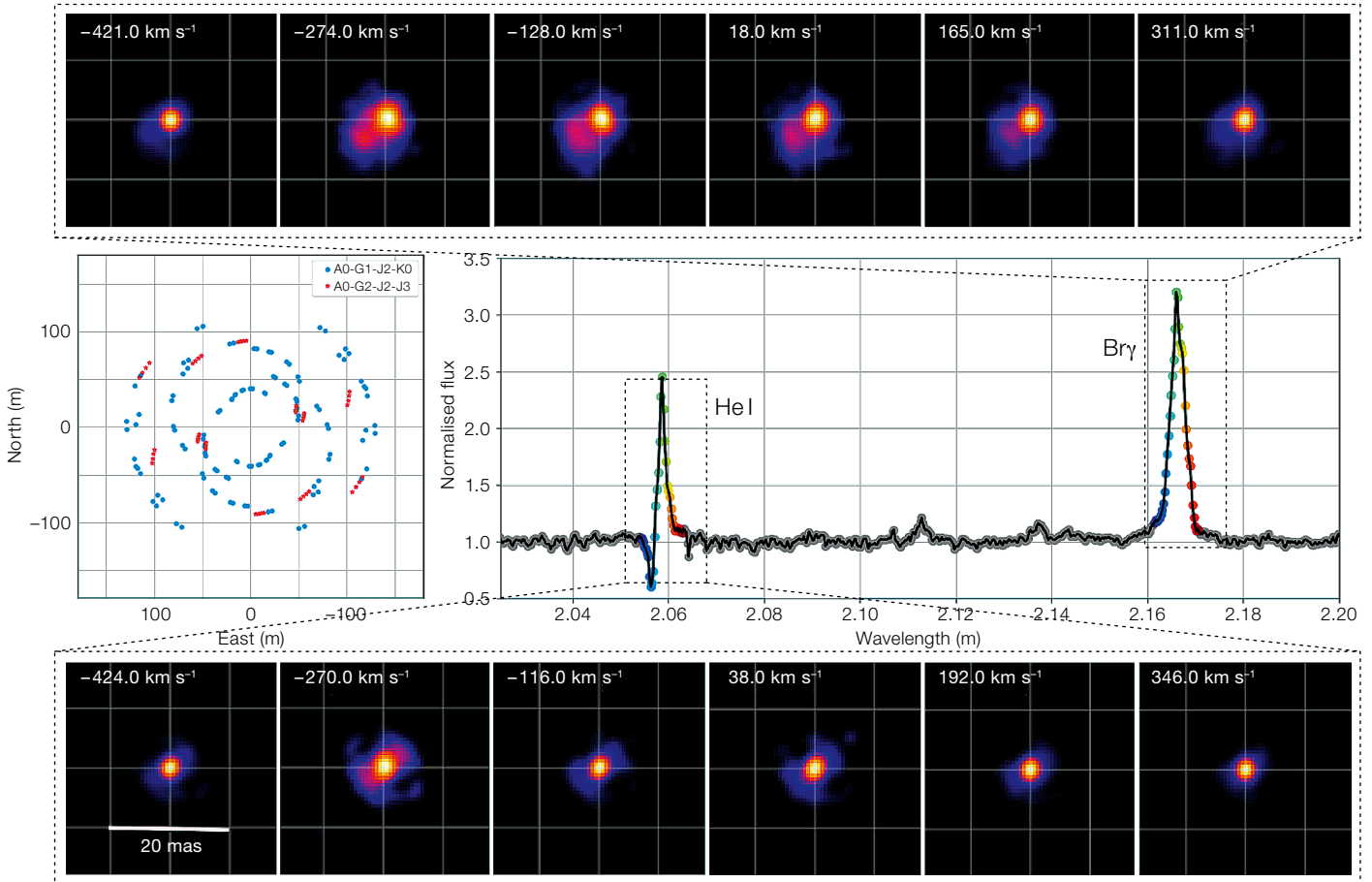rian (yellow) and relativistic (white) orbits of S2 amounts to 12 arcminutes. Bottom right: Reconstructed image from the first detection of Sgr A* by GRAVITY on 21 September 2016. The slight elongation is due to the geometry of the observatory projected on sky and is not intrinsic to the source.

Dynamics around the Galactic Centre black hole

Probing the gravitational potential around the Galactic Centre black hole Sgr A* (for example, Genzel et al., 2010) has been the primary science case and design driver of the instrument, hence the name GRAVITY (Paumard et al., 2008). The stellar orbits in the Galactic Centre are thus far perfectly Keplerian and give the best estimate of the black hole mass and its distance from Earth. The S stars within one arcsecond of Sgr A* provide ideal test particles, probing space-time in the vicinity of the black hole. With GRAVITY we want to detect general relativity effects in the orbits of those stars as deviations from Keplerian motion. S2 is the best-suited star for this experiment known so far.

Sgr A* is also surrounded by an inflow/outflow region known to exhibit flares: outbursts of energy that occur approximately once per day. The short timescale and large-amplitude brightness variations indicate that the flaring occurs a few Schwarzschild radii from the central mass. If confirmed this means the flares are additional probes for measuring the gravitational potential near the event horizon.

The Galactic Centre observations provide a good illustration of the various GRAVITY subsystems: the very bright M1 supergiant GCIRS 7 is picked up by the star separators to feed the CIAO infrared wavefront

Figure 4. (Above) Interferometric imaging of η Car. Middle left: UV coverage of the GRAVITY observations. Middle right: Normalised GRAVITY spectrum of η Car. Top (bottom): Six of the reconstructed images across the Brγ (HeI) line.

sensors; the blue supergiant GCIRS 16C (K = 9.8) feeds the fringe-tracker; and S2 and Sgr A* feed the science channel. Another nearby star serves as a local calibrator. S2 and GCIRS 16C show closure phases close to zero and visibilities around unity, indicating that they are isolated and unresolved (i.e., ideal astrometric references).

The Galactic Centre observations began in September 2016 with fireworks. The very first long exposures detected a moderate flare from Sgr A* (K = 15), with visibility and phase signatures that are typical for a binary system. Reconstructed images (Figure 3) revealed two objects in the interferometric beam: Sgr A* in its flaring state and S2. Since the initial observations, we have been monitoring Sgr A* on a monthly basis. Surprisingly, we detected the infrared counterpart of Sgr A* at all times in various brightness states. At the same time we followed S2 over its orbit with a measurable day-to-day motion.

The continuous monitoring during 2017 provides us with the astrometric baseline necessary for the detection of general relativistic deviations in S2's orbit. Only GRAVITY and the VLTI will allow the detection of S2's Schwarzschild precession soon after the pericentre flyby in spring 2018.

As we anxiously await the pericentre approach, we are constantly improving the instrument calibration and data reduction. Based on signal-to-noise calculations we are confident that in the near future, the observations will reach K ~ 19 sensitivity and contrast ratios of a few hundred. This additional increase in sensitivity will hopefully permit the detection of faint stars — which are predicted to exist based on stellar density extrapolations — with orbital periods lasting a few years or even a few months. If found, these stars could allow the detection of higher-order relativistic perturbations such as Lense-Thirring precession and frame dragging, and ultimately

provide a direct measurement of the black hole's spin.

Spectro-imaging of Eta Carinae at milli-arcsecond resolution

Eta Carinae (η Car) is one of the most intriguing luminous blue variables in the Galaxy. Models of its radiation from infrared to X-ray wavelengths imply that its core contains a binary star. The stellar wind from the secondary star creates a cavity inside the wind from the primary. Using the array of ATs, we imaged η Car with GRAVITY in February 2016. The high spectral resolution mode (R = 4000) allowed us to map η Car's wind-wind collision zone in atomic hydrogen (Brγ at 2.1661 μm) and, for the first time, in

atomic helium (He I at 2.0587 μm; Figure 4). The first and last image of each series reveal the continuum image of η Car, a compact structure of 5 milliarcseconds in size. This is the primary wind (Weigelt et al., 2016).

The GRAVITY data also confirm the presence of the wind-wind collision cavity observed with the VLTI instrument Astronomical Multi-BEam combineR, AMBER (Weigelt et al., 2016) at a velocity of −275 km s^{-1}. The bright arc-like feature in the south-east, observed at blue-shifted velocities, could be part of the hot wind due to a shock between the cavity arms after the most recent periastron passage in 2014 (Madura et al., 2013). The He I images show how ultraviolet photons from the secondary star ionise the wind from the primary. These images illustrate GRAVITY's imaging capabilities, with six simultaneous baselines and the full *K*-band at high spectral resolution. It reveals the stellar and wind parameters of large stars like η Car, and ultimately predicts their evolution and fate.

Towards dual-field astrometry

The dual-field design of GRAVITY paves the way for interferometric narrow-angle astrometry (Shao & Colavita, 1992). Differential phase measurements between the fringe-tracker and science channels remove most sources of systematic uncertainty. However, one needs to measure the differential optical path delay between the two fringes by means of GRAVITY's metrology system. The fundamental limitation becomes the atmospheric fluctuations, which — for separations of a few arcseconds — average out to about 10 microarcseconds within minutes. Reaching such accuracy will allow, for example, the detection of the reflex motion of a low-mass star (0.1–0.5 $M_\odot$) due to the presence of an Earth-mass planet on a one-year orbit.

In that respect, the well-studied binary GJ 65 AB, 2.68 pc from the Sun, is promising. Its two very-low-mass M-dwarf components (~ 0.12 $M_\odot$ each; Kervella et al., 2016) orbit each other in 26.28 years with a semi-major axis of 2.05 arcseconds. We observed GJ 65 AB repeatedly with the AT array and GRAVITY between
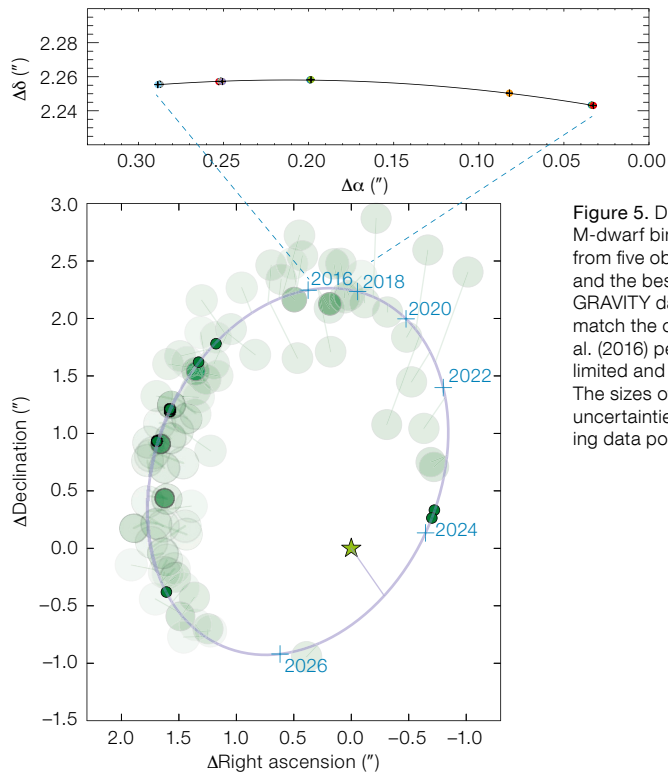

Figure 5. Dual-beam astrometry of the M-dwarf binary GJ 65. Top: Astrometry from five observing epochs in 2016–2017 and the best quadratic fit (black) to the GRAVITY data. Bottom: The GRAVITY data match the orbit of GJ 65 from Kervella et al. (2016) perfectly well, based on seeing limited and adaptive optics observations. The sizes of the discs represent the uncertainties of the single telescope imaging data points.

August 2016 and October 2017. Our measurements (Figure 5) show an unprecedented accuracy of ~ 50 microarcseconds, and we detect the orbital acceleration. Further observations will be able to detect Jovian planets around nearby M-dwarf binaries such as GJ 65. The detection of Earth-like planets requires improved modelling and correction of the various systematic errors in order to achieve the design goal of 10-microarcsecond accuracy.

Accretion and ejection mechanisms in the binary T Tauri system S CrA

We have observed both components of the binary system S Coronae Australis (S CrA North and South) using GRAVITY and the UT array. This system (130 pc from Earth) consists of an early G-type primary (*K* = 6.6) and an early K-type secondary star (*K* = 7.3). Each component is a classical T Tauri star. With an apparent separation of 1.4 arcseconds, we have been able to employ the dual-field mode, thereby doubling the flux in each channel compared to single-field observations. We swapped between the two components to observe both at high resolution (*R* = 4000).

Our *K*-band continuum observations show a disc around each component with half-flux radii of about 0.1 astronomical units (au), and inclinations and position angles identical within the uncertainties of a few degrees. This reveals that the two stars formed from the fragmentation of a common disc. Moreover, the variations of the interferometric quantities as a function of wavelength through the emission lines from atomic hydrogen in S CrA North reveal complex dynamics in a compact region (0.06 au) located well within the dust sublimation radius. This region is twice as large as the inner truncation radius below which accretion onto the star is magnetically driven. This suggests the coexistence of a stellar wind with magnetospheric accretion onto S CrA North (Figure 6).

A high-mass X-ray binary at microarcsecond accuracy

The high-mass X-ray binary (HMXB) BP Cru consists of a slowly rotating neutron star (GX 301-2) accreting from the wind of its blue hypergiant companion (Wray 977; Kaper et al., 2006). Like most X-ray binaries, the orbital system size
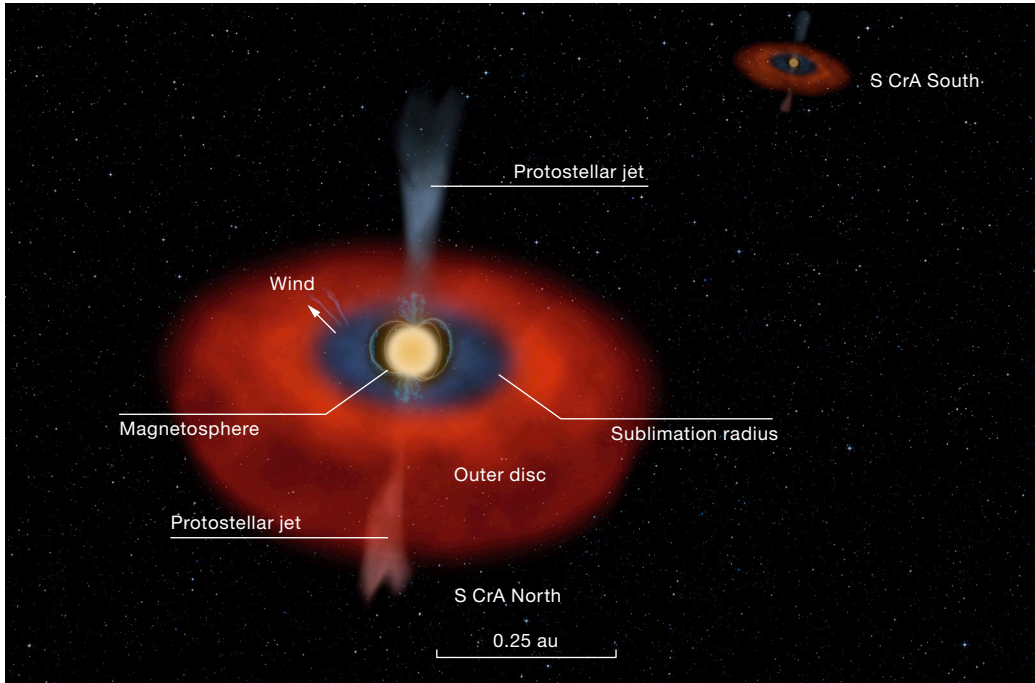
Figure 6. Artist's impression of the S CrA binary T Tauri system. GRAVITY data reveal details at an unprecedented small scale. The northern component shows a complex mixture of ejection and accretion between the scale of the magnetosphere (0.03 au) and of the sublimation radius (0.1–0.15 au). The spin axes of the two accretion discs are almost aligned, suggesting that they formed from a common precursor disc. The contrast between the large separation (1.4 arcseconds or about 200 au) and the small size of each component has been artificially reduced in this artist's impression.

(< 1 mas) is smaller than the resolution of even the largest optical/near-infrared interferometers. However, using the technique of spectral differential interferometry, it is possible to obtain spatial information on much smaller scales of a few microarcseconds. BP Cru was observed

with GRAVITY and the UTs in high spectral resolution ($R = 4000$) with a total on-source integration of 2100 s. The differential visibility and phase across the Brγ line of atomic hydrogen (shown in Figure 7) resolve the centroid shift and extension of the flux distribution as a

function of velocity. The data reveal an extended (~ 4 R_*) and distorted wind around the donor star, as well as the possible presence of a gas stream previously predicted from the X-ray lightcurve (Leahy & Kostka, 2008). The GRAVITY phase errors of 0.2 degrees correspond to a
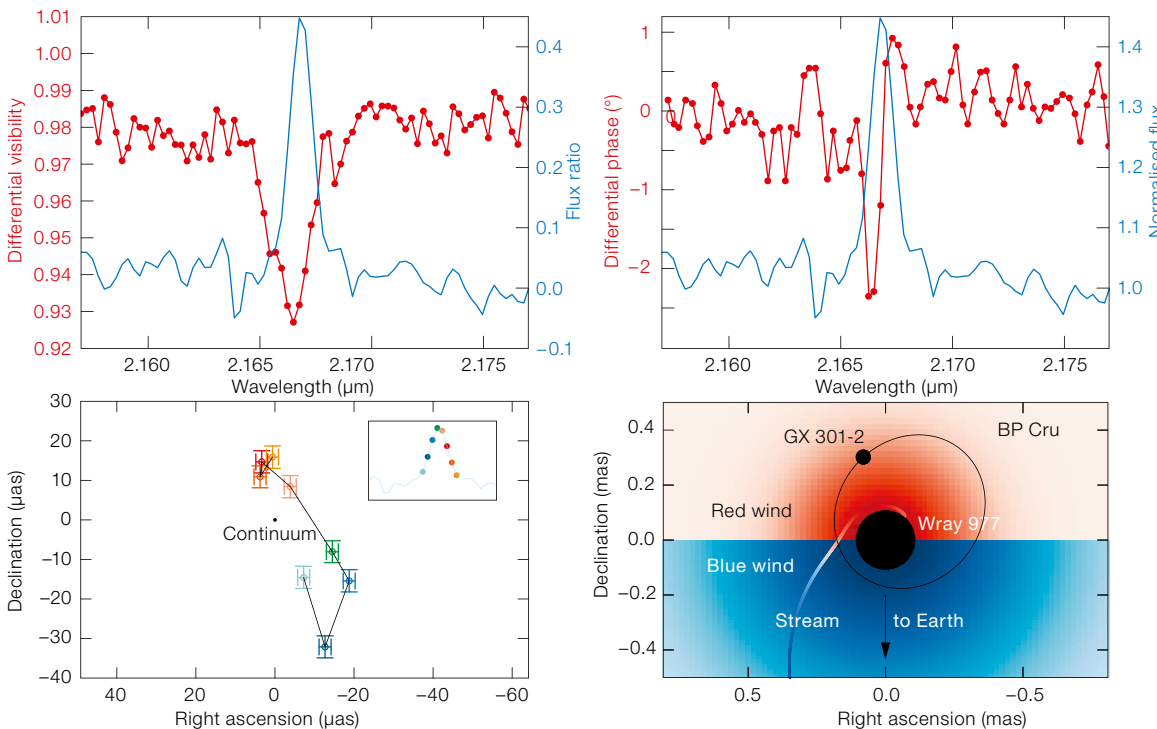

Figure 7. Tracing the inner region of the HMXB BP Cru. The upper figures show the differential visibility (left) and phase (right) for the UT1–UT4 baseline across the Brγ line as well as the flux profile. Their combination measures the centroid position and extension of the flux distribution as a function of velocity, shown in the lower left panel, with typical errors of 2 microarcseconds. The data show an extended and distorted wind around the donor star, with a blue side about two times larger than the red side. Further, the data support the presence of a gas stream (bottom right), as predicted from X-ray data to explain the asymmetry probed by the differential phases.
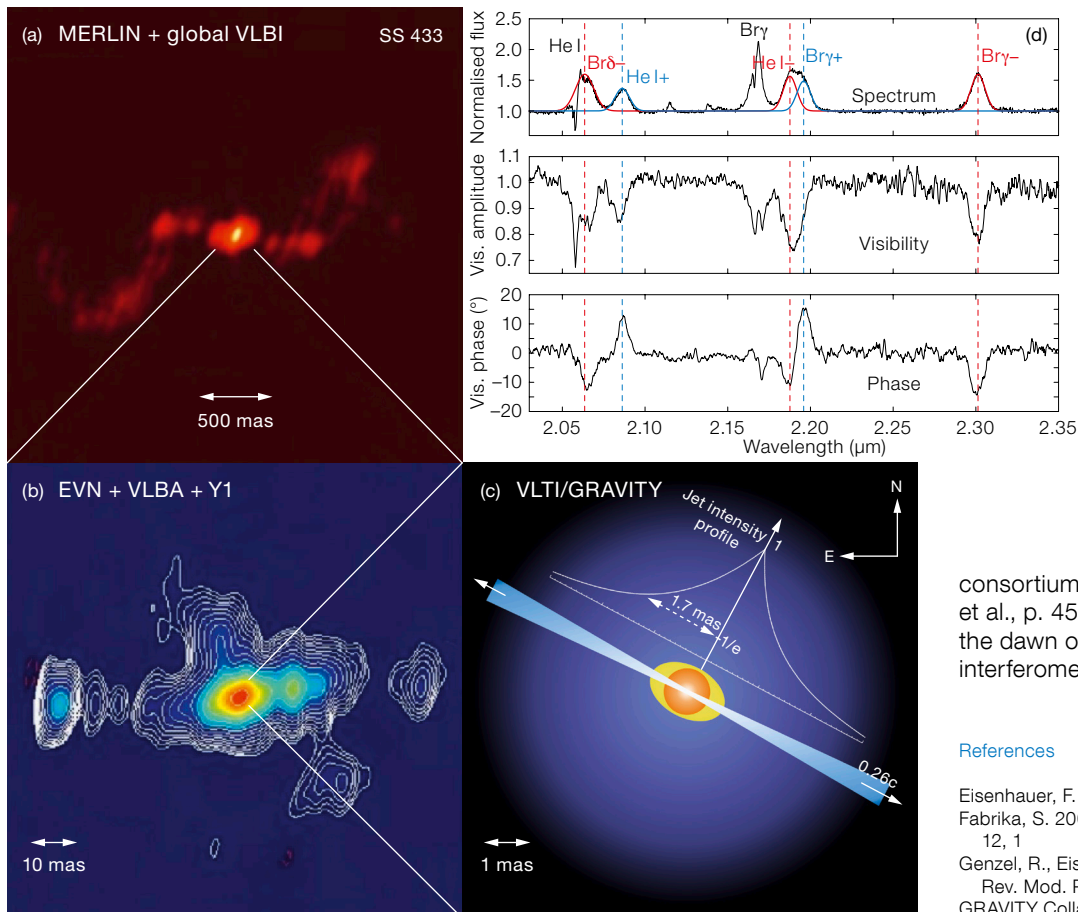
Figure 8. The microquasar SS433. The large-scale structure of the relativistic jets of SS 433 has been previously studied with radio interferometry using the Multi-Element Radio Linked Interferometer Network (MERLIN), the Very Long Baseline Interferometer (VLBI) and the European VLBI Network (EVN) (panels a and b). For the first time GRAVITY has spatially resolved the wind and redshifted ($v/c \sim 0.26$) emission lines from the baryonic jet. The K-band spectrum from GRAVITY shows several lines from the jet (shown in panel d as red/blue for the receding/approaching jets) in Brγ, Brδ and He I, as well as stationary lines from Brγ and HeI. Differential visibilities and phases are seen across all lines (d), allowing models of the emission regions at sub-milliarcsecond scales (c).

centroid difference of 2 microarcseconds for a 100-metre baseline.

First optical interferometry of a microquasar

The high sensitivity of GRAVITY allowed the first near-infrared interferometric observation of a microquasar at a submilliarcsecond scale. The well-known X-ray binary SS 433 ($K = 8.2$, $V = 13.0$) is the only source in the galaxy known to accrete persistently in excess of its Eddington rate. The super-critical accretion drives massive winds and powerful precessing relativistic jets (Fabrika, 2004).

With 80 minutes of on-source exposure time with the UTs in high spectral resolution, GRAVITY simultaneously resolved all of these components. The winds were seen in the continuum emission (partially resolved at a size of ~ 0.8 mas) with evidence for bipolar outflows seen in the stationary (i.e., non-jet) Brγ emission

line. Differential interferometry at several redshifted emission lines ($v/c \sim 0.26$) revealed the spatial structure of the relativistic jets (Figure 8).

While the large-scale structure of the jets had previously been studied at radio wavelengths (Paragi et al., 2001), we have spatially resolved its baryonic jet emission lines (Margon et al., 1979) for the first time. The jet emission peaks surprisingly close to the binary, and is well-modelled with a resolved (~ 2 mas) intensity profile that is exponentially decreasing.

GRAVITY has entered the science phase

The results presented in this article are only selected examples of early science from GRAVITY. The wider community has benefited from GRAVITY's performance since 2016, with two Science Verification runs in June and September and open-time operation since October 2016. With additional results from PIs outside of the

consortium (Mérand et al., p. 16; Kraus et al., p. 45), The Messenger celebrates the dawn of a new era for optical interferometry.

References

Eisenhauer, F. et al. 2011, The Messenger, 143, 16
Fabrika, S. 2004, Astrophys. & Space Phys. Rev., 12, 1
Genzel, R., Eisenhauer, F. & Gillessen, S. 2010, Rev. Mod. Phys., 82, 3121
GRAVITY Collaboration: Abuter, R. et al. 2017a, A&A, 602, A94
GRAVITY Collaboration: Garcia Lopez, R. et al. 2017b, A&A, 608, A78
GRAVITY Collaboration: Petrucci, P. O. et al. 2017c, A&A, 602, L11
GRAVITY Collaboration: Waisberg, I. et al. 2017d, ApJ, 844, 72
Kaper, L., van der Meer, A. & Najarro, F. 2006, A&A, 457, 595
Kervella, P. et al. 2016, A&A, 593, A127
Leahy, D. A. & Kostka, M. 2008, MNRAS, 384, 747
Madura, T. I. et al. 2013, MNRAS, 436, 3820
Margon, B. et al. 1979, ApJ, 233, 63
Paragi, Z. et al. 2001, Ap&SS Suppl., 276, 131
Paumard, T. et al. 2008, *The Power of Optical/IR Interferometry: Recent Scientific Results and 2nd Generation Instrumentation*, ed. Richichi, A., Delplancke, F., Paresce, F. & Chelli, A., (Berlin Heidelberg: Springer-Verlag), 313
Shao, M. & Colavita, M. M. 1992, A&A, 262, 353
Weigelt, G. et al. 2016, A&A, 594, A106